Decay scheme of ^{11}Be

D. J. Millener, D. E. Alburger, and E. K. Warburton
Brookhaven National Laboratory, Upton, New York 11973

D. H. Wilkinson
Brookhaven National Laboratory, Upton, New York 11973
and University of Sussex, Falmer, Brighton, England

(Received 3 May 1982)

In a reinvestigation of the β decay of ^{11}Be, formed in the ^{9}Be$(t,p)^{11}$Be reaction at $E_t=3.0$ MeV, the unique first-forbidden β-ray transition to the 4445 keV, $J^\pi=\frac{5}{2}^-$ state of ^{11}B has been found with a branching intensity of $0.054\pm0.004\%$ and $\log f_1 t=10.93\pm0.03$. The previously unobserved 692-keV γ-ray branch in the $7978\rightarrow7286\rightarrow0$ cascade following the β feeding of the ^{11}B 7978-keV state has also been measured as 0.85% and limits were placed on other γ branches from the 7978-keV level. Revised values are given for various other β- and γ-ray branching ratios. Shell model calculations are made using the full $1\hbar\omega$ basis for the positive-parity states and $0\hbar\omega+2\hbar\omega$ for the negative-parity states. The calculated electromagnetic decays of positive-parity states in ^{11}B are compared with experiment. The first-forbidden β-decay matrix elements involved in the decay of ^{11}Be to the lowest four states of ^{11}B are calculated and the resultant decay rates are compared with experiment. The question of meson exchange corrections to the $\frac{1}{2}^+\rightarrow\frac{1}{2}^-$ β decay is considered.

[RADIOACTIVITY ^{11}Be [from ^{9}Be(t,p)]: measured E_γ, I_γ, $\gamma-\gamma$ coincidence; Ge(Li) and NaI(Tl) detectors: deduced β- and γ-ray branches, logft values; compared with theory.]

I. INTRODUCTION

The one-body operators which enter in first-forbidden β decay depend on the coordinate $\vec{r}$ or momentum $\vec{p}$ of a single nucleon. The matrix elements of such operators between low-lying nuclear states are generally strongly hindered with respect to single-particle estimates and are thus difficult to calculate reliably. Tests of techniques for calculating such matrix elements are important given the current interest in meson exchange current contributions to the timelike component of the axial vector current and to parity mixing in light nuclei. The two-body operators entering these processes are closely related and there are strong indications that a major part of their effect is that of an effective one-body operator $(\vec{\sigma}\cdot\vec{p})$ and that the ratio of the two-body to the one-body matrix elements is remarkably insensitive to nuclear structure.[1-4]

Particular interest has centered on $0^+\leftrightarrow0^-$ β transitions since only the matrix elements of γ_5 and $\vec{\sigma}\cdot\vec{r}$ enter and it is to the γ_5 matrix element that large pion exchange current contributions are expected. However, rather more examples of $J^+\leftrightarrow J^-$, $J\neq0$ transitions have been measured in light ($A<30$) nuclei and it is found[5] that the matrix elements of the rank zero operators usually dominate in such transitions. Thus, an omnibus comparison of experiment and theory for these transitions will provide an important test of our ability to calculate the rank 0 matrix elements. Crucial to this test is the calculation of rank 1 matrix elements in $J_i\neq J_f$ decays, for this will provide us with a test of our ability to separate out the rank 1 contributions to $J_i=J_f$ decays.

Since ^{11}Be has a non-normal parity ground state ($J^\pi=\frac{1}{2}^+$) (Ref. 6) the β transitions with the highest energy release in the decay of ^{11}Be, to the low-lying negative parity levels of ^{11}B, are first forbidden in character. Also the high-energy release ($Q_0=11.51$ MeV) means that it is possible to observe several first-forbidden branches in the same nucleus. With the present observation of the unique first-forbidden branch to the 4445-keV level of ^{11}B, four first-

forbidden branches are now known, including the two largest branches to the $J^\pi = \frac{3}{2}^-$ ground state (55%) and the $\frac{1}{2}^-$ first-excited state (31%). Thus, ^{11}Be decay is a rich arena for testing techniques for calculating the matrix elements under discussion.

As a further test of matrix elements connecting states of different parity, we consider the γ decays between normal and non-normal parity states in ^{11}B in some detail.

An alternative approach to separating the rank zero and rank one contributions to the decay rates involves a measurement of the electron-neutrino angular correlation. Such a measurement for the ^{11}Be decay to the ^{11}B $\frac{1}{2}^-$ state is described in the following paper (hereafter referred to as II).[7] The electron-neutrino correlation is also sensitive to the particular combination of rank one matrix elements making up the rank one contribution to the decay rate and some information on this question is also obtained in II.

II. EXPERIMENTAL METHODS AND RESULTS

Previous experimental investigations of the β decay of ^{11}Be to γ-ray emitting states of ^{11}B, first[8] using the ^{11}B$(n,p)^{11}$Be reaction to form the activity, and later[9–11] the ^{9}Be$(t,p)^{11}$Be reaction, were limited by the necessity of hand carrying the activated samples from the target room of the 3.5-MV Van de Graaff to the counting area. Thus, attempts to detect certain weak β-ray branches, particularly the unique first-forbidden branch to the 4445-keV $J^\pi = \frac{5}{2}^-$ state of ^{11}B, did not succeed, partly because of insufficient statistical accuracy. Several years ago a general purpose "rabbit" target-transfer system, similar to two such systems[12] at the Brookhaven MP tandem Van de Graaff facility, was installed at the 3.5-MV Van de Graaff, and a timer-programmer[13] was made available for automatic control. Aside from the much longer runs that are possible with this system, the prospects for better γ-ray data were also improved by (1) even larger volume and better resolution Ge(Li) detectors than before, (2) overall analyzing systems of greater gain stability, and (3) more refined techniques and better reference sources for establishing the efficiency versus γ-ray energy for Ge(Li) detectors. All of these factors made a convincing case for reinvestigating the β decay of ^{11}Be in order to search for several interesting β^- and γ-ray transitions in the decay scheme.

The ^{11}Be activity was produced in the ^{9}Be$(t,p)^{11}$Be reaction by bombarding a 4.63-mg/cm^2 Be foil with 3.0-MeV tritons from the 3.5-MV Van de Graaff. The rabbit system transported the activated foil into the control room for counting. For singles γ-ray measurements a large volume Ge(Li) detector was placed on one side of the rabbit line, with 6 mm of Pb and 6 mm of brass interposed to absorb β rays and low-energy γ rays. γ-γ coincidences were studied by placing a 12.5-cm diameter by 15-cm thick NaI(Tl) detector on the other side of the rabbit line, with a 6-mm thick brass absorber interposed to exclude β rays. Beta spectra and β-γ coincidences were recorded using a Pilot B scintillation crystal 7.1 cm in diameter by 5.8 cm long cemented with epoxy onto an RCA 4524 photomultiplier tube.

The cycle of operations consisted of 6 sec of target irradiation, a pause of 8 sec followed by transfer of the rabbit, counting for 14 sec, and return of the rabbit for another irradiation. The 8-sec pause allowed for the decay of 0.8-sec ^{8}Li, produced in the ^{9}Be$(t,\alpha)^{8}$Li reaction, an activity that emits high-energy β rays and produces a background of bremsstrahlung radiation.

Gamma-ray singles data were accumulated for a total elapsed time of 28 hours using an irradiating beam current of 0.65 μA. A portion of the γ-ray spectrum is given in Fig. 1 which clearly shows the presence of the 4445-keV full-energy peak due to ground-state γ rays following the unique first-forbidden β-ray branch to that state of ^{11}B. The corresponding single- and double-escape peaks were also observed.

Another γ-ray transition that had not been observed previously in the ^{11}Be singles spectrum had an energy of 692 keV. In order to demonstrate its suspected assignment to the 7978$\rightarrow$7286$\rightarrow$0 cascade, the γ-γ coincidence arrangement was used. When a bias of >2.3 MeV was placed on the output of the NaI(Tl) detector the lines occurring in the Ge(Li) coincidence γ-ray spectrum taken in a 15-h run were those of the 692-, 1771-, and 2124-keV transitions, as shown in Fig. 2, plus the 511-keV annihilation γ rays. Upon moving the NaI(Tl) γ-ray bias up to >6.3 MeV a coincidence run of 7 h duration showed only the 692- and 511-keV peaks, the former with the intensity expected at the higher bias on the NaI(Tl) detector output. It was clear from the coincidence data and the γ-ray sums that the 692-keV γ ray belongs to the 7978$\rightarrow$7286$\rightarrow$0 cascade. These data confirmed as well the previous assignment of the 1771-keV γ ray to the 6792$\rightarrow$5020$\rightarrow$0 cascade.

Calibration of the Ge(Li) detector relative efficiency versus γ-ray energy was made with sources

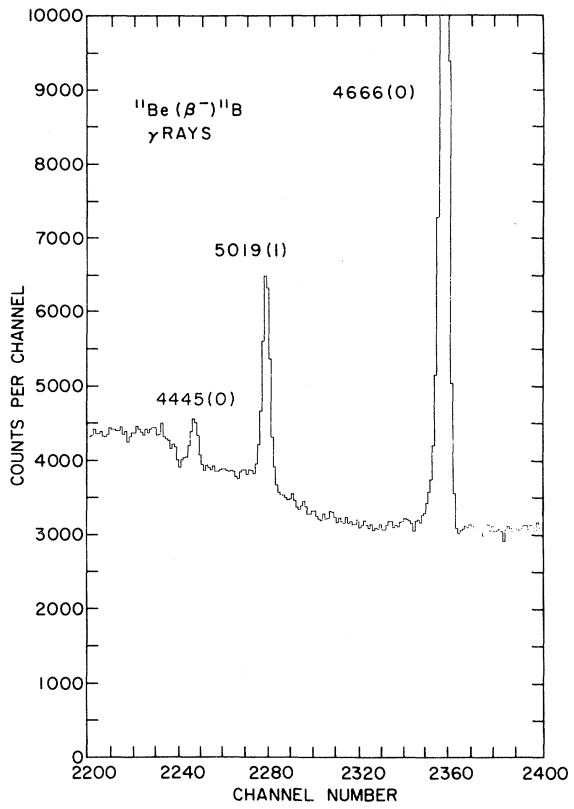

FIG. 1. Portion of the γ-ray spectrum from ^{11}Be decay showing clear evidence for the 4445-keV γ-ray transition. Gamma-ray energies are in keV. The numbers in parentheses denote full-energy (0) and one-escape (1) peaks.

of ^{56}Co or ^{152}Eu placed next to the rabbit line in separate runs. The γ-ray intensities from these activities are known accurately.[14] Energies of the γ rays in ^{11}Be decay were based in part on a previous precision measurement[15] of the 2124.473(27)-keV γ ray.

Table I lists the γ-ray energies, relative intensities, and transition assignments in ^{11}B derived from the present work. This information can be used to calculate the ^{11}B excitation energies and the γ-ray branching ratios from these states as given in Table II.

The β branching ratio to the ^{11}B ground state was determined from the β-γ coincidence data described in II using the technique described in a recent investigation of ^{21}F.[16] The absolute γ-detection efficiency needed to interpret this result was provided by the ^{20}F(β^-)^{20}Ne β-γ coincidence data obtained at the same time and also described in II. This measurement gave 0.370 ± 0.025 as the fraction of betas in coincidence with 2125-keV γ decays. Averaging this result with the previous determination[10] of 0.33 ± 0.03 gives 0.355 ± 0.018 for our adopted value. Combining this result with the γ intensities of Table I, we find a β-branching ratio of $31.4\pm1.8\%$ to the 2125-keV level. By normalizing to this branching ratio, the other β branches may be derived from the γ-ray intensity data. The results are listed in Table III which also gives the logft values. The logf_1t for the branch to the 4445-keV state follows the definition by Warburton, Garvey, and Towner.[17] The proposed decay scheme of ^{11}Be is given in Fig. 3 and includes previous results[11] on the β decay to the 9875-keV α-particle emitting state of ^{11}B.

III. SHELL MODEL CALCULATIONS

We consider first the structure of the low-lying energy levels of $A=11$ with $T=\frac{1}{2}, \frac{3}{2}$. Then we proceed to discuss the electromagnetic decays of the lowest positive-parity levels and finally the β decay of ^{11}Be with emphasis on the first-forbidden transitions.

A. Negative parity levels: $0\hbar\omega$

The $\frac{3}{2}^-_1$, $\frac{1}{2}^-_1$, $\frac{5}{2}^-_1$, and $\frac{3}{2}^-_2$ levels of ^{11}B at 0, 2125, 4445, and 5020 keV, respectively, are populated in first-forbidden β transitions from the decay of ^{11}Be and also in the electromagnetic decays of the positive-parity states of interest to us. These four levels have dominant p^7 configurations and we use the Cohen and Kurath (8−16)2BME interaction[18] to provide wave functions in a $0\hbar\omega$ shell-model calculation. The essential features of these wave functions are given in Table IV. The maximum spatial symmetry $[f]=[43]$, equivalently $(\lambda\mu)=(13)$, dominates in all wave functions. The $\frac{1}{2}^-$ and $\frac{5}{2}^-$ wave functions have mainly $L=1$ and $L=2$, respectively, while the two $\frac{3}{2}^-$ wave functions are basically orthogonal admixtures of $L=1$ and $L=2$. The (13) component of the $\frac{3}{2}^-_1$ wave function has a large overlap with the J-projected SU(3) wave function[19] with $K=\frac{3}{2}$, consistent with a description in terms of the Nilsson model; similarly the $\frac{3}{2}^-_2$ wave function is largely $K=\frac{1}{2}$.

B. Positive parity levels: $1\hbar\omega$

A comprehensive study of the positive parity-states of ^{11}B calculated in a full $1\hbar\omega$ basis has been

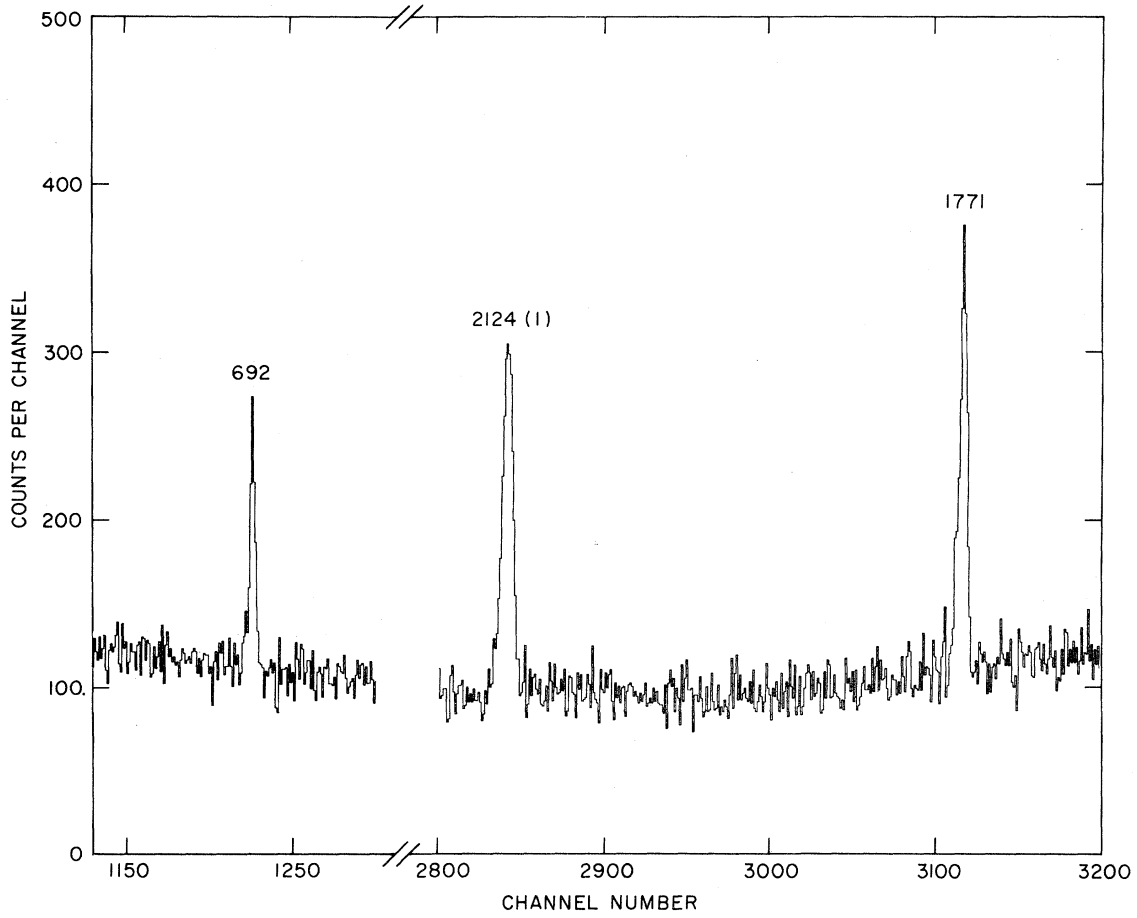

FIG. 2. Portions of the ^{11}Be γ-ray spectrum in coincidence with a NaI(Tl) detector biased at $E_\gamma \geq 2.3$ MeV. When the bias was raised to ≥ 6.3 MeV the 1771- and 2124-keV components were absent, but the 692-keV peak remained.

made by Teeters and Kurath.[20] Our treatment is essentially the same except for some minor changes in the two-body matrix elements and single-particle energies; we use the (8−16)2BME interaction for the p shell and a modified Millener-Kurath interaction[21] to calculate all the remaining two-body matrix elements. The differences between our results and those of Teeters and Kurath are small except possibly for almost degenerate levels of the same spin, a situation which does not apply to the levels of direct interest to us in this investigation.

To interpret the structure of the low-lying positive-parity levels Teeters and Kurath expressed the wave functions in a weak-coupling basis. Our wave functions are expressed in an SU(3) basis (it is simple to make a transition to the weak-coupling basis). As in the case of the weak-coupling basis the bulk of each wave function is given in terms of a few basis functions. The (42) and (23) representations give most of each wave function with the (42) representation dominant (see Fig. 5). The (42) configuration results from coupling a particle in the sd shell to the dominant (22) symmetry of lowest p-shell states of the ^{10}B core

$$(22)\times(20)\rightarrow(42)(23)(31)(04)(12)(20)\,. \quad (1)$$

The simplest approximation for the $A=11$ positive-parity states is pure (42) with [43] symmetry for $T=\frac{1}{2}$, implying equal parentage to isospin zero and one of the core, and [421] symmetry for $T=\frac{3}{2}$. In this limit there is no allowed ($\sigma\tau$ cannot change [f]) or first-forbidden [$(13)\times(10)\not\rightarrow(42)$] decay of ^{11}Be. Since $\vec{r}$ and $\vec{p}$, in an oscillator model, transform under SU(3) as $(10)+(01)$, the $1\hbar\omega$ representations connected to the dominant p^7 configurations are to be found in the following products:

$$\begin{aligned}&(13)\times(10)\rightarrow(23)(04)(12)\,,\\&(21)\times(10)\rightarrow(31)(12)(20)\,.\end{aligned} \quad (2)$$

TABLE I. Energies and relative intensities of ^{11}B γ rays from ^{11}Be(β^-)^{11}B. Numbers in parentheses denote the uncertainties in the least significant figure. N denotes a γ-ray energy calculated from the excitation energies given in Table II.

γ energy (keV)	Transition (keV)	Relative intensity
692.31(10)	7978→ 7286	0.097(3)
1185.98(N)	7978→ 6792	<0.011
1171.31(30)	6792→ 5020	0.740(40)
2124.473(27)	2125→ 0	100.000
2346.64(N)	6792→ 4445	<0.007
2895.30(40)	5020→ 2125	0.227(8)
2957.10(N)	7978→ 5021	<0.01
3532.34(N)	7978→ 4445	<0.007
4443.90(50)	4445→ 0	0.153(8)
4665.90(40)	6792→ 2125	5.115(140)
5018.98(40)	5020→ 0	1.316(46)
5851.47(42)	7978→ 2125	6.006(240)
6789.81(50)	6792→ 0	12.618(620)
7282.92(N)	7286→ 0	<0.17
7974.73(N)	7978→ 0	5.342(400)

It is these non-(42) representations which are important in first-forbidden β decay and $E1$ transitions; spurious center-of-mass states exist with these quantum numbers and care must be taken to eliminate them. Teeters and Kurath have emphasized that the small $s^{-1}p^8$ components in the positive-parity wave functions play a very important role in $E1$ transitions; the $s^{-1}p$ particle-hole configuration is (10) in character while in the case of $p^{-1}(sd)$ the effective interaction favors (21) over (10) in forming the low-lying positive-parity levels. For $\frac{1}{2}^+$, $T=\frac{1}{2}$ the s-hole admixture can be quite large since the hole couples to the tightly bound ^{12}C ground state and the s-hole configuration therefore comes relatively low in energy; Teeters and Kurath suggested[22] that evidence for this $s^{-1}p^8$ component could be found in inelastic electron scattering, and subsequent experiments[23] at Darmstadt confirm their predictions.

C. Negative parity states: $2\hbar\omega$

The lowest $2\hbar\omega$ configuration is expected to be the $p^5(sd)^2$ (71) configuration occurring in the product

$$(31)\times(40)\rightarrow(71)(52)(33)(14)\,. \qquad (3)$$

In a calculation which includes the $p^5(sd)^2$, $p^6(pf)$, and $s^{-1}p^7(sd)$ configurations with $(\lambda\mu)=(71)$, (52), (33), and (14), $S=\frac{1}{2}, \frac{3}{2}$ for (71) (52) and $S=\frac{1}{2}$ only for (33) (14), the lowest states are 80% (71). The lowest state is predicted to be $\frac{3}{2}^-$ and may be an important component in the 8.56-MeV $\frac{3}{2}^-_3$ level of ^{11}B. It is at this excitation energy or just above that the p^7 model fails to produce enough levels. How-

TABLE II. ^{11}B level energies and γ-ray branching ratios from ^{11}Be(β^-)^{11}B. Numbers in parentheses indicate the uncertainties in the least significant figure.

Initial level[a] (keV)	Final level (keV)	Branching ratio (%) Present	Previous[b]	Adopted
2124.693(27)	0	100	100	100
4444.89(50)	0	100	100	100
5020.31(30)	0	85.3(7)	86.6(10)	85.6(6)
	2125	14.7(7)	13.4(10)	14.4(6)
6791.80(30)	0	68.3(11)	66.0(15)	67.5(11)
	2125	27.7(11)	30.0(15)	28.5(11)
	4445	<0.04	<0.5	<0.04
	5020	4.0(3)	4.1(9)	4.0(3)
7285.51(43)	0		87.0(20)	87.0(20)
7977.84(42)	0	46.7(20)	46.0(14)	46.2(11)
	2125	52.5(20)	54.0(14)	53.2(12)
	4445	<0.06	<1.0	<0.06
	5020	<0.09	<1.0	<0.09
	6792	<0.10	<1.4	<0.10
	7286	0.85(4)		0.85(4)

[a]Based on the γ-ray energies in Table I.
[b]The least squares average of the ratios quoted in Ref. 6.

TABLE III. β-ray branches of ^{11}Be ($J^\pi=\frac{1}{2}^+$, $t_{1/2}=13.81$ sec, $Q_\beta=11.509$ MeV) and logft values. The numbers in parentheses indicate the uncertainties in the least significant figure.

^{11}B level (keV)	J^π	Branching ratio (%)	logft (except as noted)
0	$\frac{3}{2}^-$	54.7(20)[a]	6.830(16)
2125	$\frac{1}{2}^-$	31.4(18)	6.648(25)
4445	$\frac{5}{2}^-$	0.054(4)	10.93(3)[b]
5020	$\frac{3}{2}^-$	0.282(20)	7.934(31)
6792	$\frac{1}{2}^+$	6.47(45)	5.938(30)
7286	$(\frac{3}{2},\frac{5}{2})^+$	<0.03	>8.04
7978	$\frac{3}{2}^+$	4.00(30)	5.576(33)
9875	$\frac{3}{2}^+$	3.1(4)[c]	4.04(8)[c]

[a]From the relative γ-ray intensities of Table I and $I_{2125\gamma}/I_{\text{total}\beta}=0.355(18)$.
[b]logf_1t.
[c]From the relative γ-ray intensities of Table I and $I_\alpha/I_{2125\gamma}$ of Ref. 11.

ever, to describe levels in this region near the ^{7}Li+α and ^{8}Be+t thresholds may require more clustering than is present in the shell-model wave functions, as is indicated in $\alpha+\alpha+t$ cluster model calculations.[24]

Our interest is not in these levels *per se* but rather in those $2\hbar\omega$ admixtures in the wave functions of the four lowest negative-parity levels which can contribute directly to $E1$ or first-forbidden matrix elements, i.e., those representations which occur in the products

$$\begin{aligned}&(42)\times(10)\rightarrow(52)(33)(41)\,,\\&(23)\times(10)\rightarrow(33)(14)(22)\,.\end{aligned}\tag{4}$$

We must next ask which representations are most strongly coupled to p^7 configurations by the effective interaction (V). The strongest components of V which connect states differing by $2\hbar\omega$ are the (20) SU(3) tensor components of the central force. Thus representations in the following products concern us

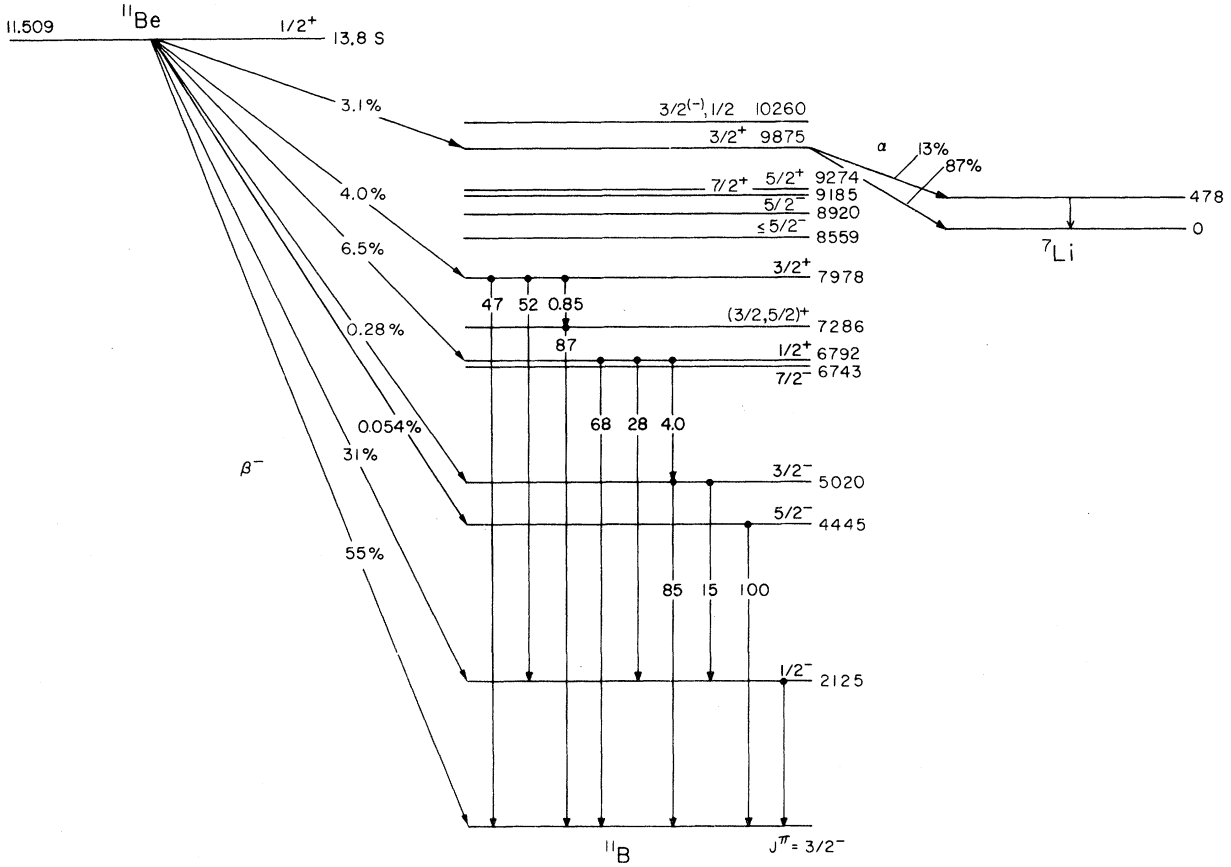

FIG. 3. Proposed decay scheme of ^{11}Be including the new β-ray branch to the ^{11}B 4445-keV level and revised values for other β^- and γ-ray branches.

TABLE IV. Negative parity wave functions calculated with the Cohen and Kurath (8−16)2BME interaction.

State		Intensity of each $(\lambda\mu)\equiv[f]$ (%)				Amplitudes of (13) components		
J_n^π	E_n (keV)	(13)	(21)	(02)	(10)	$L=1$	$L=2$	$L=3$
$\frac{3}{2}_1^-$	0	82.28	13.54	3.07	1.11	0.768	−0.483	
$\frac{3}{2}_2^-$	5020	89.81	5.40	3.86	0.93	0.492	0.810	
$\frac{1}{2}_1^-$	2125	94.67	4.21	0.95	0.17	0.973		
$\frac{5}{2}_1^-$	4445	92.42	6.17	1.25	0.16		0.945	0.115

$$(13)\times(20)\rightarrow(33)(14)(22)(03)(11)\ ;\ S=\tfrac{1}{2}\ ,$$
$$(21)\times(20)\rightarrow(41)(22)(30)(03)(11)\ ;\ S=\tfrac{1}{2},\ \tfrac{3}{2}\ . \tag{5}$$

Including only (33) and (14) configurations as we have done may cause some distortion of the predominantly $0\hbar\omega$ wave functions since representations coupling strongly to the (21) $0\hbar\omega$ configuration are omitted. Also there are $4\hbar\omega$ configurations which couple strongly to the $2\hbar\omega$ configurations, and so on. This is a process slowly convergent in the unperturbed energy of the admixed configurations and has been studied mainly in cluster-model calculations. Nevertheless we feel that our $2\hbar\omega$ calculation is sufficient to illustrate the role played by $2\hbar\omega$ configurations in transitions between positive- and negative-parity levels (see Fig. 4).

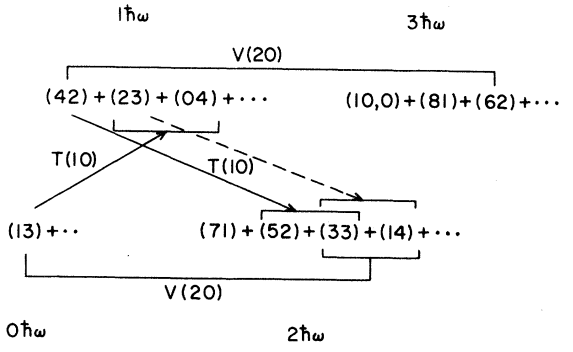

FIG. 4. Connections between representations important in the wave functions of low-lying $A=11$ states. The (13) and (42) configurations are the "large" components in the negative- and positive-parity states, respectively. In a few cases the (23) component may also be regarded as large (see Table V). Other components are "small." The operators V represent the strongest part of the effective interaction [central (20) tensor] while the transition operator T represents $\vec{r}$, $[\vec{r},\vec{\sigma}]^k$, $\gamma_5(\sim\vec{\sigma}\cdot\vec{p})$ or $\vec{\alpha}(\sim\vec{p})$ with the appropriate isospin dependence. T connects large to small.

In passing we note that the $E2$ operator connecting configurations differing by $2\hbar\omega$ transforms as $(20)+(02)$ so that the $p^6(pf)$ and $s^{-1}p^7(sd)$ components of the strongly admixed $2\hbar\omega$ configurations strongly influence $E2$ transitions between levels with dominantly p^7 configurations. For example, the $\frac{5}{2}_1^-\rightarrow\frac{3}{2}_1^-$ $E2$ transition, experimentally[25] 7.1 ± 0.8 W.u. (Weisskopf units[26]) in strength, is modestly enhanced from 3.7 W.u. in the p^7 calculation to 6.2 W.u. when $2\hbar\omega$ admixtures are included.

D. Electromagnetic transitions in ^{11}B

The general band structure of the $T=\frac{1}{2}$ positive-parity states in ^{11}B is illustrated in Fig. 5, where $B(M1)$ and $B(E2)$ values for transitions between such states are displayed. The wave functions of these states have large (42) components (Fig. 5) with various possible $[f]SKL$ values ($[f]S=[43]\frac{1}{2}$ or $[421]\frac{1}{2}$, $\frac{3}{2}$, and $K=0$ or 2), e.g., the large $B(E2)$ values connect states with similar $[f]SK$ structures.

We consider in detail the γ decay of the lowest positive-parity states of ^{11}B—6792 keV ($\frac{1}{2}^+$), 7286 keV ($\frac{5}{2}^+$), 7978 keV ($\frac{3}{2}^+$), 9185 keV ($\frac{7}{2}^+$), and 9274 keV ($\frac{5}{2}^+$)—and also the decay of the analog of the ^{11}Be ground state—12 560 keV ($\frac{1}{2}^+$). A comparison of shell-model predictions to experiment for the relevant electromagnetic transitions is made in Table V.

In this paper we have reported the observation of the 7978→7286 $M1$ transition, the only transition between positive-parity levels so far observed, and set an upper limit on the strengh of the 7978→6792 $M1$ transition. The order of magnitude of the reduced transition strengths involving these three levels can be easily understood from the basic features

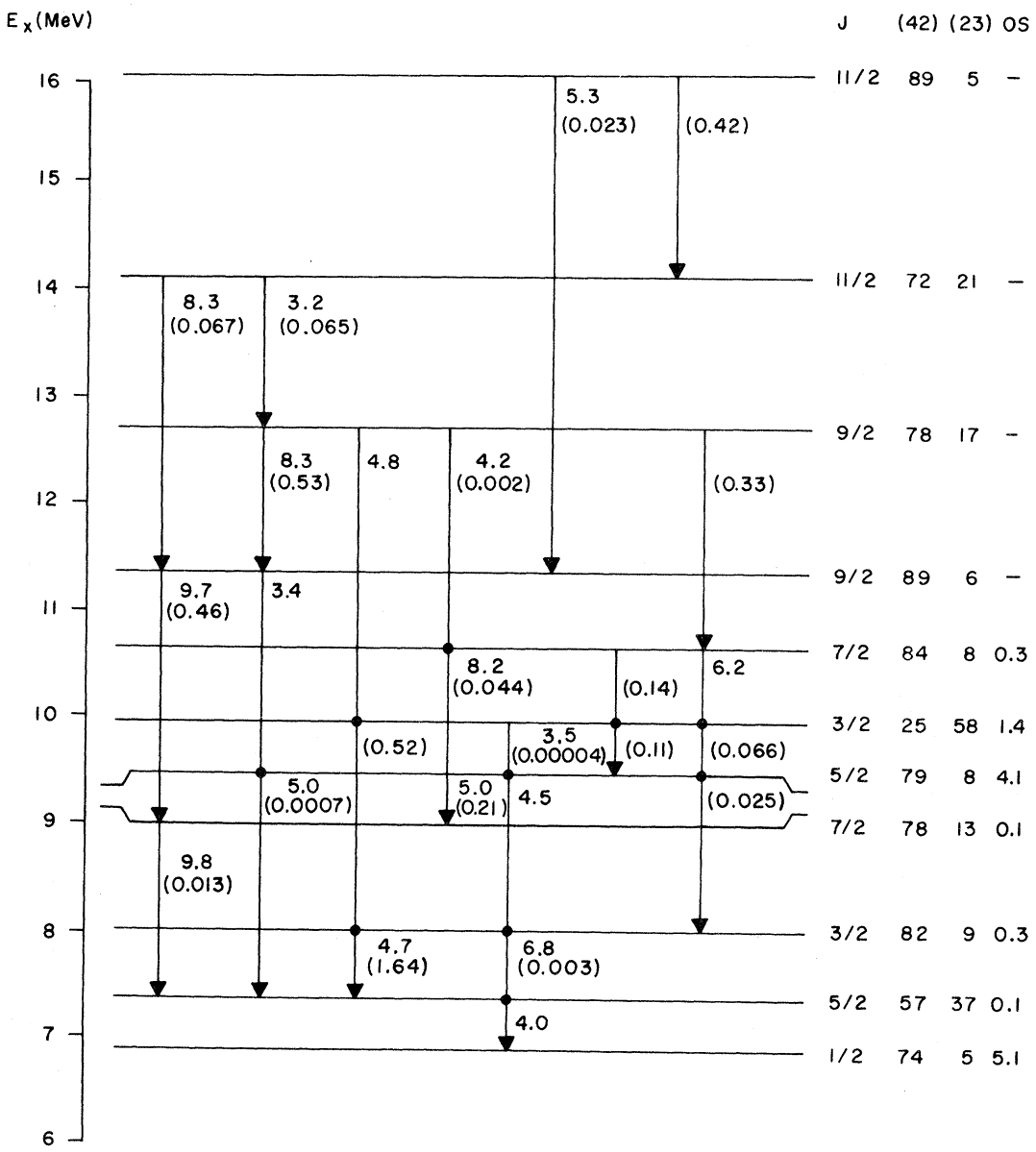

FIG. 5. Calculated $B(E2)$ and $B(M1)$ values in Weisskopf units (Ref. 26) for transitions involving positive parity states in ^{11}B. The $B(M1)$ values are given in parentheses. For $E2$ transitions the isoscalar effective charge is double the bare value and the radial matrix elements are computed using oscillator wave functions with $b=1.6528$ fm. Only $B(E2)>3$ W.u. are shown. The percentage intensities of the (42), (23), and 0s-hole configurations are given at the right of the figure for each level.

of the wave functions—dominant (42) components (Fig. 5), $L=0$ (88%) for $J=\frac{1}{2}$ and $L=2$ (93% and 90%) for $J=\frac{5}{2}$ and $J=\frac{3}{2}$. For the (42) components $K=0$ dominates (42% and 72% of the total wave function for $J=\frac{5}{2}$ and $J=\frac{3}{2}$). We note that the ordering of the $J=\frac{5}{2}$ and $J=\frac{3}{2}$ states is as we would expect for $L=2$, $S=\frac{1}{2}$ states split by the one-body spin-orbit force. For the strong $\frac{3}{2}^+_1 \rightarrow \frac{5}{2}^+_1$ $M1$ transition there is excellent agreement between theory and experiment (Table V) while the calculated value for the weak (L forbidden) $\frac{3}{2}^+ \rightarrow \frac{1}{2}^+$ transition is an order of magnitude less than the experimental upper limit ($<3.8\times10^{-2}$ W.u.).

For transitions involving a change of parity (mainly $E1$ transitions) we consider first calcula-

TABLE V. Comparison of shell-model predictions to experiment for electromagnetic transitions in ^{11}B.

$J^\pi T \rightarrow J_f^\pi$ ($T_f=\frac{1}{2}$)	$E_i \rightarrow E_f$ (keV)	Quantity	Transition strength[a] Experiment[b]	Theory[c]
$\frac{1}{2}^+, \frac{1}{2} \rightarrow \frac{3}{2}^-$	6792 → 0	$B(E1)$	$2.5(3)\times10^{-3}$	2.5×10^{-3}
		$B(M2)$		0.59
$\rightarrow\frac{1}{2}^-$	→2125	$B(E1)$	$3.2(4)\times10^{-3}$	3.2×10^{-3}
$\rightarrow\frac{5}{2}^-$	→4445	$B(M2)$	<30	0.18
$\rightarrow\frac{3}{2}^-$	→5020	$B(E1)$	$8.3(11)\times10^{-3}$	10×10^{-3}
$\frac{5}{2}^+, \frac{1}{2} \rightarrow \frac{3}{2}^-$	7286 → 0	$B(E1)$	$7.7(5)\times10^{-3}$	11×10^{-3}
		$B(M2)$		1.63
		$B(E3)$		11.5
$\rightarrow\frac{1}{2}^-$	→2125	$B(M2)$	<43	0.88
$\rightarrow\frac{5}{2}^-$	→4445	$B(E1)$	$8.3(16)\times10^{-3}$	10×10^{-3}
$\rightarrow\frac{3}{2}^-$	→5020	$B(E1)$	$22.2(15)\times10^{-3}$	12×10^{-3}
$\frac{3}{2}^+, \frac{1}{2} \rightarrow \frac{3}{2}^-$	7978 → 0	$B(E1)$	$3.1(4)\times10^{-3}$	8.7×10^{-3}
$\rightarrow\frac{1}{2}^-$	→2125	$B(E1)$	$9.1(12)\times10^{-3}$	5.3×10^{-3}
$\rightarrow\frac{5}{2}^-$	→4445	$B(E1)$	$<4.7\times10^{-5}$	9.6×10^{-5}
$\rightarrow\frac{3}{2}^-$	→5020	$B(E1)$	$<1.4\times10^{-4}$	8.4×10^{-4}
$\rightarrow\frac{1}{2}^+$	→6792	$B(M1)$	$<3.8\times10^{-2}$	3.1×10^{-3}
$\rightarrow\frac{5}{2}^+$	→7286	$B(M1)$	1.42(20)	1.64
$\frac{7}{2}^+, \frac{1}{2} \rightarrow \frac{3}{2}^-$	9185 → 0	$B(M2)$	0.6(3)	0.31
		$B(E3)$		6.4
$\rightarrow\frac{5}{2}^-$	→4445	$B(E1)$	$7.2(23)\times10^{-3}$	11×10^{-3}
$\rightarrow\frac{7}{2}^-$	→6743	$B(E1)$	$8.2(27)\times10^{-3}$	6.2×10^{-3}
$\frac{5}{2}^+, \frac{1}{2} \rightarrow \frac{3}{2}^-$	9274 → 0	$B(E1)$	$2.0(4)\times10^{-3}$	1.8×10^{-2}
$\rightarrow\frac{5}{2}^-$	→4445	$B(E1)$	$48(10)\times10^{-3}$	4.0×10^{-3}
$\rightarrow\frac{3}{2}^-$	→5020	$B(E1)$	$<5\times10^{-3}$	2.4×10^{-3}
$\rightarrow\frac{7}{2}^-$	→6743	$B(E1)$	$63(13)\times10^{-3}$	23×10^{-3}
$\frac{1}{2}^+, \frac{3}{2} \rightarrow \frac{3}{2}^-$	12560 → 0	$B(E1)$	$15(9)\times10^{-3}$	71×10^{-3}
$\rightarrow\frac{1}{2}^-$	→2125	$B(E1)$	$6.6(43)\times10^{-3}$	52×10^{-3}
$\rightarrow\frac{3}{2}^-$	→5020	$B(E1)$		5.6×10^{-3}

[a]The transition strengths $B(EL)$ and $B(ML)$ are in Weisskopf units (Ref. 26).
[b]See the Appendix and Table II.
[c]Bare g factors are used for all magnetic transitions. No effective charge is used for $E1$ transitions. For $E3$ transitions the isoscalar effective charge is double the bare value. The radial matrix elements are computed using oscillator wave functions with $b=1.6528$ fm. Only a few of the stronger $B(M2)$ and $B(E3)$ values are given, these for ground state transitions.

tions limited to $0\hbar\omega$ and $1\hbar\omega$ for the negative and positive parity states, respectively; i.e., the spaces used by Teeters and Kurath.[20] Teeters and Kurath have emphasized that the $E1$ matrix elements depend sensitively on the small $s^{-1}p^8$ components in the positive-parity wave functions. [Some of the two-body matrix elements involving the $0s$ orbit have the wrong sign in the Teeters and Kurath calculation, the result of a misunderstanding between D. Kurath and one of us (D.J.M.). The conclusions of Ref. 20 do not change upon using a corrected set of two-body matrix elements but naturally some of the calculated $E1$ matrix elements change somewhat on account of the delicate cancellations involved.] This is shown clearly in Fig. 6, where the strengths of the three $E1$ transitions involved in the decay of the 6792-keV $\frac{1}{2}^+$ level are plotted as a function of the single-hole energy of the $0s$ orbit. Also plotted is the $0s$-hole content of the $\frac{1}{2}^+$ level. For a single hole energy of 18.5 MeV, slightly larger than the 17 MeV of Teeters and Kurath's set 2 of single-particle energies, there is good agreement between theory and experiment for all three $E1$ transitions. We now fix the $0s$-hole energy at 18.5 MeV and calculate transition strengths for all known decays from positive- to negative-parity levels. Theory and experiment are compared in Table V. The agreement is fair with the notable exception of the $E1$ decays from the analog of the ^{11}Be ground state which are predicted to be far too strong. These transitions from the $\frac{1}{2}^+_1$, $T=\frac{3}{2}$ level especially concern us since essentially the same matrix elements enter directly into the calculation of first-forbidden β-decay transitions from ^{11}Be. As Teeters and Kurath have observed,[20] these large $E1$ matrix elements may indicate that there is too much parentage of the ^{10}Be ground state in the initial and final states. This can be verified by making use of

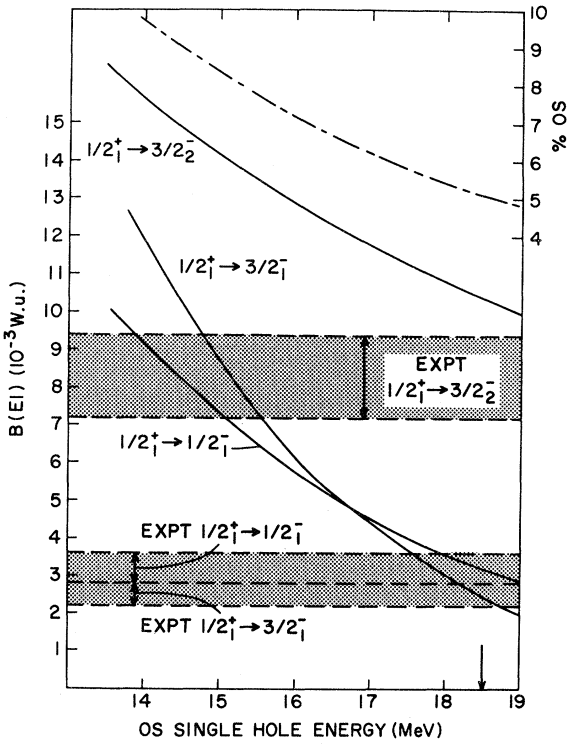

FIG. 6. $B(E1)$ transition strengths (left-hand scale) from the 6792-keV $\frac{1}{2}^+$ level of ^{11}B as a function of the energy of the $0s$-hole energy. The uppermost curve on the figure gives the percentage of $0s$-hole configuration in the $\frac{1}{2}^+$ shell-model wave function (right-hand scale). A value of 18.5 MeV is used for the $0s$-hole energy in the construction of Table V.

the one-body density matrix elements (OBDME) and single-particle matrix elements (SPME) in Table VI to calculate the contributions from individual orbits to the matrix element of the single particle operator T,

$$\langle J_f T_f M_{T_f}||T||J_i T_i M_{T_i}\rangle = \langle T_i M_{T_i} \Delta T M_{\Delta T} \mid T_f M_{T_f}\rangle \times \sum_{j_1 j_2} \frac{\hat{j}_1 \hat{\frac{1}{2}}}{\hat{\Delta J}\hat{\Delta T}} \langle j_1 \tfrac{1}{2}|||T|||j_2 \tfrac{1}{2}\rangle \langle J_f T_f|||(a^\dagger_{j_1}\tilde{a}_{j_2})^{\Delta J \Delta T}|||J_i T_i\rangle , \quad (6)$$

where ΔJ and ΔT are the space-spin and isospin ranks of T. The isospin factor in the coefficient of the one-body density matrix element is unity for β decay (operator $1/\sqrt{2}\tau^{\pm}$) and $\sqrt{2}$ for electromagnetic transitions (operator τ_3). The low-lying p-shell states of the ^{10}Be core are the 0^+ ground state and 2^+ states at 3.37 and 5.96 MeV so that the dominant contributions to the $\frac{1}{2}^+$; $T=\frac{3}{2} \rightarrow \frac{1}{2}^-_1$ and $\frac{1}{2}^+$; $T=\frac{3}{2} \rightarrow \frac{3}{2}^-_1$ $E1$ matrix elements are from the $1s_{1/2}p_{1/2}$ and $1s_{1/2}p_{3/2}$ density matrix elements, respectively, which arise almost entirely from the main ($>80\%$) ^{10}Be$(0^+,1)\otimes 1s_{1/2}$ component of the $T=\frac{3}{2}$ wave function. In each case the $d_{5/2}p_{3/2}$ contribution provides some cancellation, the two

TABLE VI. One-body density matrix elements[a] for ^{11}Be β decay.

$J_iT_i \rightarrow J_fT_f$	ΔJ	(j_1j_2) $1s_{1/2}p_{1/2}$	$d_{3/2}p_{1/2}$	$1s_{1/2}p_{3/2}$	$d_{3/2}p_{3/2}$	$d_{5/2}p_{3/2}$	$d_{5/2}p_{1/2}$	$p_{1/2}os_{1/2}$	$p_{3/2}os_{1/2}$
$\frac{1}{2}^+, \frac{3}{2} \rightarrow \frac{1}{2}^-, \frac{1}{2}$	0	−0.4857			0.0390			−0.0089	
	1	−0.8320	−0.0019	0.0146	−0.0217	−0.0616		0.0148	−0.0237
$\rightarrow \frac{3}{2}_1^-, \frac{1}{2}$	1	−0.0083	0.0006	−0.7172	0.0899	−0.1163		−0.0496	0.0215
	2		0.0016	−0.9383	−0.0558	−0.3032	−0.0455		0.0000
$\rightarrow \frac{3}{2}_2^-, \frac{1}{2}$	1	−0.0205	−0.0821	−0.1750	−0.0257	0.0447		−0.0053	−0.0329
	2		0.0253	−0.2038	0.0263	0.1097	−0.2457		−0.0135
$\rightarrow \frac{5}{2}_2^-, \frac{1}{2}$	2		0.0750	0.0175	−0.1135	0.1063	−0.0430		−0.0324
$\rightarrow \frac{1}{2}_1^-, \frac{3}{2}$	1	−0.8100	−0.0000	−0.0629	−0.0089	−0.2203		0.0423	0.0540

One body operator (T)	Single particle matrix elements[b]							
irC_1	$-\sqrt{2/9}$	$\sqrt{10/9}$	$-\sqrt{4/9}$	$\sqrt{2/9}$	$\sqrt{2}$		$-\sqrt{1/3}$	$\sqrt{2/3}$
$ir[C_1,\sigma]^0$	$\sqrt{2/3}$			$\sqrt{10/3}$			1	
$ir[C_1,\sigma]^1$	$-\sqrt{4/9}$	$-\sqrt{5/9}$	$\sqrt{2/9}$	$\sqrt{16/9}$	1		$\sqrt{2/3}$	$\sqrt{1/3}$
$ir[C_1,\sigma]^2$		$-\sqrt{1/15}$	$-\sqrt{2/3}$	$\sqrt{4/15}$	$\sqrt{7/5}$	$-\sqrt{8/5}$		1

[a] $\langle J_iT_i||(a^\dagger_{j_1}\tilde{a}_{j_2})^{\Delta J\Delta T=1}||J_fT_f\rangle$; $\tilde{a}_{jm\,1/2m_t}=(-)^{j-m+1/2-m_t}a_{j-m\,1/2-m_t}$; Brink and Satchler convention (Ref. 35) for the reduced matrix elements; radial wave functions positive at the origin together with $[i^lY_{l\frac{1}{2}},]^j$. Note that the initial state has been written on the left.

[b] $\langle j_1||T||j_2\rangle\hat{j}_1/\hat{\Delta J}$ given in units of the oscillator parameter b. The matrix elements needed to compute w', x', and u' can be obtained (for $R=3.25$ fm, $b=1.6528$ fm) by multiplying the entries in the table by 0.7494 ($1sp$), 0.8229 (dp), and 0.8720 ($p0s$).

main contributions giving a reasonably good approximation to the full $E1$ matrix element. The $d_{5/2}p_{3/2}$ OBDME comes mainly from the ^{10}Be$(2_1^+,1)\otimes d_{5/2}$ component in the $\frac{1}{2}^+;T=\frac{3}{2}$ wave function. The $d_{5/2}$ single-particle energy is constrained by the energy of the second-excited state at 1.78 MeV in ^{11}Be which is thought to have $J^\pi=\frac{5}{2}^+$ and in our calculation comes 1.39 MeV above the ground state. The use of Woods-Saxon wave functions in place of harmonic oscillator wave functions brings about a reduction in the $B(E1)$ values, by factors of ~ 1.7 and ~ 1.4 for the transitions to the ground and first-excited states, respectively. [To estimate the contribution of the unbound $s_{1/2}$ proton to the dominant $s\rightarrow p$ term in Eq. (6) we have made an extrapolation through zero binding energy.] The effect of $2\hbar\omega$ admixtures in the negative-parity wave functions is calculated to be small. While $3\hbar\omega$ admixtures in the positive-parity wave functions may cause some reduction in the $E1$ rates mainly through a normalization effect on the $1\hbar\omega$ component (Fig. 4), we do not expect significant changes from this source. Thus at present we do not understand the strong $E1$ transitions from the $\frac{1}{2}^+;T=\frac{3}{2}$ level in ^{11}B.

One possibility that should be considered is the influence of isospin mixing on the decay of the $\frac{1}{2}^+;T=\frac{3}{2}$ level in ^{11}B, for if SU(3) and SU(4) were good symmetries the $\frac{1}{2}_1^+;T=\frac{3}{2}$ level would be degenerate with a $\frac{1}{2}^+;T=\frac{1}{2}$ level with the same space-spin structure, [421] (42) $L=0$, $S=\frac{1}{2}$. In our calculation two $\frac{1}{2}^+;T=\frac{1}{2}$ levels occur close to the $\frac{1}{2}^+;T=\frac{3}{2}$ level, the energies of $\frac{1}{2}_2^+;\frac{1}{2}$, $\frac{1}{2}_3^+;\frac{1}{2}$ and $\frac{1}{2}_1^+;\frac{3}{2}$ states being 12.99, 13.45, and 13.58 MeV, respectively. For slightly different choices of interaction the two $T=\frac{1}{2}$ levels can bracket the $T=\frac{3}{2}$ level. The two $T=\frac{1}{2}$ levels contain in total 54% of the [421] (42) $L=0$, $S=\frac{1}{2}$ configuration; the primary admixture, totalling 50%, is from the [421] (42) $K=0$, $L=2$, $S=\frac{3}{2}$ configuration. The $B(E1)$ values for the decay of $\frac{1}{2}_2^+;T=\frac{1}{2}$ to the $\frac{3}{2}_1^-$, $\frac{1}{2}_1^-$, and $\frac{3}{2}_2^-$ levels are calculated to be very similar in strength to those for the decay of the $\frac{1}{2}^+;T=\frac{3}{2}$ level, with the $B(E1)$ values for the decay of $\frac{1}{2}_3^+;T=\frac{1}{2}$ being about a factor of 3 weaker. If the $E1$ matrix elements for the decay of the $T=\frac{1}{2}$ and $T=\frac{3}{2}$ states are indeed comparable it follows that quite small isospin admixtures can have a considerable effect on decay of

the $T=\frac{3}{2}$ level for the case of destructive interference. Also the calculated signs of the $E1$ matrix elements for either $T=\frac{1}{2}$ state are such that if the admixture is destructive for the transition to the $\frac{3}{2}_1^-$ level then it is also destructive for the transition to the $\frac{1}{2}_1^-$ level. Thus it is possible that isospin mixing of the $\frac{1}{2}^+$ levels, for which there is some evidence,[27] could help to explain the observed decay rates of the 12.56-MeV $\frac{1}{2}^+$ level of ^{11}B. However, as will be discussed, the β decay of the ^{11}Be ground state also provides evidence that the calculated $E1$ matrix elements are too large.

An additional source of information on the $\frac{1}{2}^+$; $T=\frac{3}{2}$ wave function is the lifetime of the first-excited state of ^{11}Be ($J^\pi=\frac{1}{2}^-$). The measured[28] value of this quantity is (0.18 ± 0.06) psec, corresponding to a $B(E1)$ of 0.33 W.u. The calculated value [using the OBDME of Table VI and harmonic oscillator (HO) wave functions] is 0.011 W.u. There is a strong cancellation between the $1s_{1/2}p_{1/2}$ and $d_{5/2}p_{3/2}$ contributions. Even so, the $1s_{1/2}p_{1/2}$ contribution by itself gives only 0.08 W.u. This is a case where the observed lifetime cannot be accounted for without taking into account the low binding energies of the $1s_{1/2}$ and $0p_{1/2}$ orbits. The use of Woods-Saxon wave functions greatly increases the $p_{1/2}\rightarrow s_{1/2}$ single-particle matrix element, at the same time rendering the cancellation between the $s_{1/2}p_{1/2}$ and $d_{5/2}p_{3/2}$ contributions less effective. The calculated $B(E1)$ is increased by a factor of almost 20 to 0.21 W.u. We note that increasing the $d_{5/2}$ content of the $\frac{1}{2}^+$; $T=\frac{3}{2}$ level to decrease the calculated $T=\frac{3}{2}\rightarrow T=\frac{1}{2}$ transition rates (and increase the calculated half-life of ^{11}Be) will also decrease the $\frac{1}{2}^-$; $\frac{3}{2}\rightarrow\frac{1}{2}^+$; $\frac{3}{2}$ transition rate.

E. β decay of ^{11}Be

Our comparison between theory and experiment of the absolute decay rate utilizes the expression[29,30]

$$ft=6170 \text{ sec} , \tag{7}$$

where t is the partial half-life of the transition and

$$f=\int_1^{W_0} C(W)F(Z,W)(W^2-1)^{1/2}W(W_0-W)^2dW \tag{8}$$

In Eq. (8) W is the β energy and W_0 the disintegration energy (maximum β energy), both in units of the electron rest mass (and including the rest mass), and Z is the charge of the final nucleus. We use natural units $\hbar=c=m_e=1$. The unit of time is seconds, and of length the electron Compton wavelength, $\lambda\!\!\!^{-}_e=386.15$ fm. If only dominant terms are retained the first-forbidden shape factor can be written in the form[30,31]

$$C(W)=k(1+aW+b/W+cW^2) \tag{9}$$

and thus

$$f=k(I_0+aI_1+bI_{-1}+cI_2) , \tag{10}$$

where the integrals

$$I_n=\int_1^{W_0} W^nF(Z,W)(W^2-1)^{1/2}W(W_0-W)^2dW \tag{11}$$

are given, divided by $\lambda\!\!\!^{-}_e{}^2$ for convenience, in Table VII for the four first-forbidden transitions observed in ^{11}Be decay. The evaluation of these integrals follows procedures developed for the evaluation of unique first-forbidden decays and is fully explained elsewhere.[32] In evaluating $C(W)$ we follow the treatment of Behrens and Bühring.[33] Then

$$\begin{aligned}
k&=[\zeta_0^2+\tfrac{1}{9}w^2]+[\zeta_1^2+\tfrac{1}{9}(x+u)^2-\tfrac{4}{9}\mu_1\gamma_1u(x+u)\\
&\quad+\tfrac{1}{18}W_0^2(2x+u)^2-\tfrac{1}{18}\lambda_2(2x-u)^2]+\tfrac{1}{12}z^2(W_0^2-\lambda_2) ,\\
ka&=-\tfrac{4}{3}uY-\tfrac{1}{9}W_0(4x^2+5u^2)-\tfrac{1}{6}z^2W_0 ,\\
kb&=\tfrac{2}{3}\mu_1\gamma_1[-\zeta_0w+\zeta_1(x+u)] ,\\
kc&=\tfrac{1}{18}[8u^2+(2x+u)^2+\lambda_2(2x-u)^2]+\tfrac{1}{12}z^2(1+\lambda_2) ,
\end{aligned} \tag{12}$$

where

$$\begin{aligned}
&V=\xi'v+\xi w' , \quad \zeta_0=V+\tfrac{1}{3}wW_0 ,\\
&Y=\xi'y-\xi(u'+x') , \quad \zeta_1=Y+\tfrac{1}{3}(u-x)W_0 .
\end{aligned} \tag{13}$$

The coefficients k, ka, kb, and kc depend on the nuclear matrix elements, on W_0, and on $\xi=\alpha Z/2R$, where R is the radius of a uniformly charged sphere approximating the nuclear charge distribution. This approximation is good provided R implies the correct experimental rms size of the nucleus. We use for R the expression given by

TABLE VII. Energy integrals: $I'_n = I_n/\lambda_e^2$, where $1/\lambda_e^2 = 6.7064\times10^{-6}$ fm^{-2}.

Final state	$W_0(m_e)$	I'_0	I'_1	I'_{-1}	I'_2
$\frac{3}{2}^-_1$	23.52	1.7944	21.1553	0.1871	284.350
$\frac{1}{2}^-_1$	19.36	0.6781	6.5974	0.0582	73.079
$\frac{5}{2}^-_1$	14.82	0.1773	1.3259	0.0287	11.2606
$\frac{3}{2}^-_2$	13.70	0.1165	0.8030	0.0204	6.2786

Wilkinson (p. 938 of Ref. 29) and obtain $R=3.25$ fm for $A=11$. The parameter γ_1 is given by $[1-(\alpha Z)^2]^{1/2}$ where α is the fine structure constant. For light nuclei $\mu_1=1$, $\lambda_2=1$ are very good approximations. The nuclear matrix elements are given in terms of form-factor coefficients defined by Behrens and Bühring.[33] The nonrelativistic matrix elements are

$$\begin{aligned} w &= -R\,{}^AF^0_{011} \\ &= \lambda\sqrt{3}\langle J_fT_f||ir[C_1,\vec{\sigma}]^0\vec{\tau}||J_iT_i\rangle C\ , \\ x &= -1/\sqrt{3}R\,{}^vF^0_{110} \\ &= -\langle J_fT_f||irC_1\vec{\tau}||J_iT_i\rangle C\ , \\ u &= -\sqrt{2/3}R\,{}^AF^0_{111} \\ &= \lambda\sqrt{2}\langle J_fT_f||ir[C_1,\vec{\sigma}]^1\vec{\tau}||J_iT_i\rangle C\ , \\ z &= 2/\sqrt{3}R\,{}^AF^0_{211} \\ &= -\lambda 2\langle J_fT_f||ir[C_1,\vec{\sigma}]^2\vec{\tau}||J_iT_i\rangle C\ , \end{aligned} \tag{14}$$

where $\lambda=-C_A/C_V=1.2605$ is taken from a recent analysis of neutron beta decay,[34]

$$C=\langle T_iM_i11\,|\,T_fM_f\rangle\hat{J}_f/(\sqrt{2}\hat{J}_i)$$

for β^- decay, and the reduced matrix elements are according to the definition of Brink and Satchler.[35] The matrix elements ω', x', and u' are obtained from the definitions of w, x, and u by including in the radial integral an extra factor[33]

$$\begin{aligned} \tfrac{2}{3}I(1,1,1,1;r) &= \left[1-\frac{1}{5}\left[\frac{r}{R}\right]^2\right] \quad 0<r<R \\ &= \left[\frac{R}{r}-\frac{1}{5}\left[\frac{R}{r}\right]^3\right] \quad r>R\ . \end{aligned} \tag{15}$$

The relativistic matrix elements are

$$\begin{aligned} \xi'v &= {}^AF^0_{000} = \lambda\langle J_fT_f||\gamma_5\vec{\tau}||J_iT_i\rangle C\ , \\ \xi'y &= {}^VF^0_{101} = -\langle J_fT_f||\vec{\alpha}\vec{\tau}||J_iT_i\rangle C\ . \end{aligned} \tag{16}$$

In evaluating $\xi'v$ and $\xi'y$ the usual nonrelativistic replacements for γ_5 and $\vec{\alpha}$ can be made yielding

$$\begin{aligned} \xi'v &= -\lambda\sqrt{3}\langle J_fT_f||\frac{i}{M}[\vec{\sigma},\vec{\nabla}]^0\vec{\tau}||J_iT_i\rangle C\ , \\ \xi'y &= -\langle J_fT_f||\frac{i}{M}\vec{\nabla}\vec{\tau}||J_iT_i\rangle C\ . \end{aligned} \tag{17}$$

The conserved vector current (CVC) theory may be used[33,36] to obtain an alternative expression for $\xi'y$ in terms of x and a similar nonrelativistic matrix element involving the Coulomb field of the nucleus. Under the stronger assumption that isospin is a good quantum number one has[37]

$$\xi'y = E_\gamma x\ , \tag{18}$$

where E_γ is the energy of the γ ray from the analog of the initial state to the final state. In this case x can be related to the $B(E1)$ value for the γ-ray transition

$$|x| = [B(E1)8\pi T_i/3]^{1/2} \tag{19}$$

with $B(E1)$ in units of fm^2 deduced from

$$\Gamma_\gamma = 1.04653\ E_\gamma{}^3B(E1)\ , \tag{20}$$

where Γ_γ is in units of eV and E_γ in MeV. Use of the prescription of Damgaard and Winther[33,38] for evaluating $\xi'y$ leads to effective values of E_γ in Eq. (18) which are 350–400 keV less than E_γ for the β transitions of interest. Thus the effect of using different CVC based expressions for $\xi'y$ is small for high energy β transitions and we simply use Eq. (18). There is no basis[36] for a corresponding relationship between the axial matrix elements $\xi'v$ and w although it has sometimes been assumed that $\xi'v$ is related to $-w$ as $\xi'y$ is to x. For oscillator single-particle wave functions with $2n+l=2n'+l'\pm1$

$$\begin{aligned} &\langle (l\tfrac{1}{2})j||i\vec{\sigma}\cdot\vec{\nabla}||(l'\tfrac{1}{2})j\rangle \\ &\qquad = \mp\langle (l\tfrac{1}{2})j||i\vec{\sigma}\cdot\vec{r}||(l'\tfrac{1}{2})j\rangle/b^2 \end{aligned} \tag{21}$$

so that for a $1\hbar\omega$ initial state and a $0\hbar\omega$ final state in the calculation for ^{11}Be decay

$$\xi'v = -w/Mb^2 = -E_{\rm osc}w\ , \tag{22}$$

where $E_{\rm osc}$ is the energy of an oscillator quantum ($\hbar\omega$) in units of m_e. If $2\hbar\omega$ configurations are included the relationship expressed in Eq. (22) no longer holds[2] since the operators $\vec{\sigma}\cdot\vec{\nabla}$ and $\vec{\sigma}\cdot\vec{r}$ have different Hermitian conjugation properties [expressed in Eq. (21)]; contributions of $2\hbar\omega$ configurations will be constructive in one matrix element and destructive in the other. For single-particle wave

functions other than harmonic oscillator (HO), e.g., Woods-Saxon (WS) wave functions, the ratio of matrix elements in Eq. (21) can be significantly state dependent. The difference between HO and WS single-particle matrix elements is most marked for the $0p_{1/2}-1s_{1/2}$ matrix elements which dominate the rank-zero matrix elements in light nuclei (Fig. 7—see later).

The values of the nuclear matrix elements, defined in Eqs. (14)–(18), which are needed to evaluate the decay rates, as specified in Eqs. (10)–(13), are listed in Table VIII. Results are given for both HO and WS single-particle wave functions and the effects of $2\hbar\omega$ admixtures in the negative-parity wave functions are also considered. In each case the resulting partial decay rates $f^{(k)}$, the contribution to f from rank-k nuclear matrix elements, are given and a comparison is made with the experimental decay rates. To exhibit more clearly the contribution of each of the nuclear matrix elements we substitute for the energies W_0 and E_γ in Eqs. (12) and (13) and use the energy integrals from Table VII to obtain

$$\tfrac{1}{2}\,\tfrac{1}{1}^- \quad f^{(0)}=0.678(\xi' v+7.79w)^2 , \tag{23a}$$

$$\tfrac{3}{2}\,\tfrac{1}{1}^- \quad f^{(1)}=51.31(10.59x^2+u^2-1.59xu) ,$$

$$\tfrac{1}{2}\,\tfrac{1}{1}^- \quad f^{(1)}=13.65(10.11x^2+u^2-1.86xu) , \tag{23b}$$

$$\tfrac{3}{2}\,\tfrac{1}{2}^- \quad f^{(1)}=1.30(8.98x^2+u^2-2.32xu) ,$$

$$\tfrac{3}{2}\,\tfrac{1}{1}^- \quad f^{(2)}=47.0z^2 ,$$

$$\tfrac{5}{2}\,\tfrac{1}{1}^- \quad f^{(2)}=1.83z^2 , \tag{23c}$$

$$\tfrac{3}{2}\,\tfrac{1}{2}^- \quad f^{(2)}=1.02z^2 .$$

In deriving these expressions we have dropped some very small terms which contribute to $f^{(0)}$ and have assumed that $w'/w=x'/x=u'/u=0.7$ (equivalent to $\xi\rightarrow 0.7\xi$, $w'\rightarrow w$, etc.), a rough average of ratios calculated with HO or WS wave functions (see Table VIII).

For the transition to the ^{11}B ground state, x and u are of opposite sign and Eqs. (23b) and (23c) and Table VIII show that f receives comparable contributions from x^2, u^2, and z^2. The shell-model values give an f somewhat larger than experiment, but a modest decrease in any or all of the nuclear matrix elements would bring agreement; in fact taking x from the analog γ decay via Eqs. (19) and (20) is sufficient. The evidence discussed here and in II suggests that the shell-model value of x is too large, as was the equivalent $B(E1)$ for the analog decay. Since the isospin mixing discussed for the ^{11}B $T=\frac{3}{2}$ analog does not affect the β rate, it would seem that isospin mixing alone is insufficient to explain the $B(E1)$ values for decay of the $T=\frac{3}{2}$ ^{11}B 12.56-MeV level.

The theoretical decay rates for the transitions to the $\frac{5}{2}^-$ and second $\frac{3}{2}^-$ levels are too small. The former requires $|z|=0.36$ to reproduce the experimental value. In the case of the $\frac{3}{2}\,\frac{1}{2}^-$ transition the calculated values of u and z are very small; if x alone is to produce the experimental decay rate $|x|=0.33$ is required.

For the three transitions discussed so far there are some substantial differences between the rates calculated with WS and HO wave functions, the WS wave functions generally giving a better account of the data. However, the greatest sensitivity to the choice of single-particle wave functions occurs in the transition to the $\frac{1}{2}^-$ level for the matrix element involving the gradient operator ($\xi' v$); the effect of changes in $\xi' v$ is magnified by the cancellation between $\xi' v$ and w in the expression for $f^{(0)}$ [Eq. (23a)]. Thus, for the single-particle binding energies we have chosen the use of WS wave functions reduce $f^{(0)}$ by a factor of about 4. Certainly some effect was to be expected since the $s_{1/2}$ neutron which makes the transition is bound by only 0.5 MeV in the ^{11}Be ground state; at this binding energy the rms radius of the orbit in the WS well is about twice the HO value (see Fig. 7). Figure 7 demonstrates that the ratio of single-particle matrix elements of $\vec{\sigma}\cdot\vec{r}$ to those of $\vec{\sigma}\cdot\vec{\nabla}$ can differ significantly from the HO value of b^2 (here 2.73 fm^2), particularly for the most important $s_{1/2}\rightarrow p_{1/2}$ matrix element. Actually the ratio is rather insensitive to the binding energy, and hence the mean square radius, of the *sd* orbit (except for rather low $s_{1/2}$ binding energies), but depends sensitively on the binding energy of the p orbit. This effect can be understood for the $d\rightarrow p$ matrix by assuming that the p and d wave functions can be represented by HO wave functions with different oscillator constants (b and b', respectively). Then it can easily be shown that Eq. (21) for the ratio of matrix elements still holds; i.e., the ratio is independent of b', an effect which is clearly demonstrated in Fig. 7 where the curves for the d-p matrix element ratio track closely the mean square radius of the p orbit. In the $s\rightarrow p$ case it is a poor approximation to represent the wave function of a loosely bound s orbit by a single HO wave function. Nevertheless, the behavior of the $s\rightarrow p$ and $d\rightarrow p$ ratios is similar with the $s\rightarrow p$ ratio larger than the $d\rightarrow p$ ratio for the same binding energy of the p orbit unless the p orbit is very deeply bound. The problem is what

TABLE VIII. Nuclear matrix elements defined in Eqs. (14)–(18) and decay rates [Eq. (10)]. The contributions to f from matrix elements of each rank are given to a good approximation by Eqs. (23a)–(23c).

Final state	Quantity	Basis and single particle wave function $0\hbar\omega$ (HO)	$0\hbar\omega$ (WS)[a]	$(0+2)\hbar\omega$ (HO)
$\frac{1}{2}^-$	$w(w')$	−1.206(−0.890)	−1.182(−0.751)	−1.178(−0.853)
	$\xi' v$	35.84	22.29	30.16
	$x(x')$	0.456(0.325)	0.442(0.265)	0.453(0.321)
	$u(u')$	1.387(1.020)	1.348(0.859)	1.350(0.976)
	$\xi' y$	9.305	9.025	9.244
	$f^{(0)}$	465	116	293
	$f^{(1)}$[b]	38(24)	38(23)	37(23)
	f(exp)	140±8	$f^{(0)}$(exp)=115±18	$f^{(1)}$(exp)<35
$\frac{3}{2}^-_1$	$x(x')$	0.532(0.383)	0.474(0.288)	0.544(0.389)
	$u(u')$	−1.054(−0.799)	−0.966(−0.665)	−0.971(−0.721)
	$\xi' y$	13.08	11.65	13.36
	z	1.816	1.601	1.900
	$f^{(1)}$[b]	260(114)	209(101)	255(102)
	$f^{(2)}$	155	121	170
	f(exp)	244±9		
$\frac{3}{2}^-_2$	$x(x')$	0.158(0.112)	0.195(0.117)	−0.130(−0.092)
	$u(u')$	−0.100(−0.038)	−0.100(−0.068)	0.009(−0.003)
	$\xi' y$	2.333	2.881	−1.914
	z	−0.088	0.060	0.061
	$f^{(1)}$	0.32	0.53	0.19
	$f^{(2)}$	0.01		
	f(exp)	1.26±0.09		
$\frac{5}{2}^-$	z	0.231	0.236	0.179
	$f^{(2)}$	0.10	0.10	0.06
	f(exp)	0.24±0.02		

[a]The parameters of the Woods-Saxon well are $r_0=r_{s0}=1.194$ fm, $a_0=a_{s0}=0.625$ fm, $r_c=1.446$ fm, $V_{s0}=5.7$ MeV, with $R_i=r_i A^{1/3}$ and V_0 determined to reproduce the specified separation energy.

[b]Numbers in parentheses are calculated using values of x derived from the γ transition strength of the analog via Eqs. (19) and (20). This procedure is invalid if there is appreciable isospin mixing into the analog state.

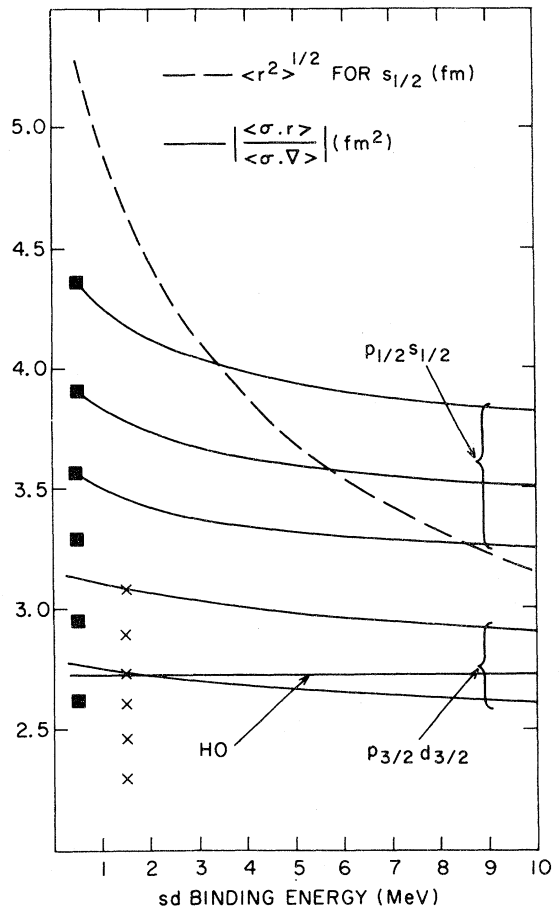

FIG. 7. Ratio of the single-particle matrix elements of the operators $\vec{\sigma}\cdot\vec{r}$ and $\vec{\sigma}\cdot\vec{\nabla}$ for Woods-Saxon ($r_0=1.198$, $a=0.625$) wave functions as a function of binding energy. The squares (crosses) give the ratio for $s\rightarrow p$ ($d\rightarrow p$) matrix elements for p-orbit binding energies of 7.1, 9.1, 11.1, 13.1, 16.1, and 20.1 MeV (top to bottom); curves showing the dependence on s- or d-binding energy are given only in some cases.

binding energy to choose for the $p_{1/2}$ orbit in ^{11}B. Generally in constructing Table VIII we chose to bind the particles for each OBDME at the separation energy determined by the parent making the dominant contribution to the OBDME. For example, for the $1s\rightarrow 0p$ rank-zero matrix elements we chose a $p_{1/2}$ binding energy of 9.1 MeV, the energy required to remove a proton from the $\frac{1}{2}^-$ level leaving ^{10}Be in its ground state. In a few cases we used the full parentage expansion with different binding energies corresponding to each parent. Although for the WS case in Table VIII $f^{(0)}$ is close to the experimental value,[7] we have yet to take into account the influence of meson exchange currents (MEC) on $\xi' v$. The MEC are expected[1,2] to enhance $\xi' v$ by about 40%.

Finally we note that the inclusion of $2\hbar\omega$ configurations in the calculation of the negative-parity wave functions does not generally lead to any improved agreement with experiment for the first-forbidden transition rates (nor did it for the electromagnetic decays of the $T=\frac{1}{2}$ positive-parity states in ^{11}B). On the contrary the interference between the $1\hbar\omega\rightarrow 0\hbar\omega$ and $1\hbar\omega\rightarrow 2\hbar\omega$ routes is almost invariably the opposite of that needed for improved agreement; e.g., the rate for the $\frac{3}{2}^-_2$ transition would be in good agreement with the experimental rate if the calculated $1\hbar\omega\rightarrow 2\hbar\omega$ contribution was of opposite sign. A single exception is the contribution to $\xi' v$ (the contribution to w is necessarily[2] in the opposite direction). However, even this improvement may be illusory since the work of Towner and Khanna[2] on ^{16}N (0^-) decay has demonstrated the importance of correlations induced in the ^{16}O ground state by the tensor force, and our restricted $2\hbar\omega$ basis for ^{11}B does not give full rein to this type of correlation.

IV. DISCUSSION

It has been suggested that the dominant rank-zero matrix element in first-forbidden beta decay, $\xi' v$, is subject to large corrections from meson exchange currents—typically[1,2] an enhancement of 40–50%. Such effects have been looked for in $0^+\leftrightarrow 0^-$ β transitions (or μ capture), which are, however, rare and usually involve the measurement of very small branches. The data on $J^+\leftrightarrow J^-$; $J\neq 0$ transitions, which are more numerous (nine cases in the light nuclei compared with two $0^+\leftrightarrow 0^-$ cases), provide an alternative means of studying MEC effects associated with the timelike component of the axial vector current if the rank-zero matrix elements dominate the transitions or if $f^{(0)}$ can be isolated. Calculations[5] suggest that the rank-zero matrix elements usually do dominate. The value of $f^{(0)}$ deduced[7] in II from a measurement of the electron-neutrino angular correlation confirms this prediction for the ^{11}Be($\frac{1}{2}^+$)$\rightarrow^{11}$B($\frac{1}{2}^-$) transition. The $J^+\leftrightarrow J^-$ transitions are thus a potentially valuable source of information on MEC effects. However, an unambiguous statement on MEC effects requires that the structure of the initial and final nuclear states be sufficiently well understood. We have emphasized that this is a difficult task since the matrix elements

of the β decay operators between low-lying nuclear levels are small; the strength lies in the ($E1, M2, \ldots$) giant resonance region of the daughter nucleus. It is clear that, although we get some encouragement from our calculations, the description of the first-forbidden branches in ^{11}Be decay is not yet satisfactory despite the fact that the ground state of ^{11}Be has an apparently simple structure. We have also pointed out that the evaluation of $\xi' v$ depends quite sensitively on the choice of single-particle wave functions. For all rank-zero matrix elements in light nuclei the $s_{1/2} \rightarrow p_{1/2}$ matrix element is the most important; however, for cases other than ^{11}Be decay the p shell is full (or nearly so) and the choice of the $p_{1/2}$ binding energy is well defined. For example, in the $^{16}\mathrm{N}(0^-) \rightarrow {}^{16}\mathrm{O}(0^+)$ transition the $s_{1/2}$ and $p_{1/2}$ binding energies can be identified with the separation energies as 2.4 and 12.1 MeV, respectively. Then the single-particle matrix elements are not very different from the HO values and the ratio exhibited in Fig. 7 is only 10% larger than the HO value. Finally, we note that attempts[39] at relativistic many-body theories suggest that the $1/M$ factor in the nonrelativistic reduction of γ_5 should be replaced by $1/\tilde{M}$, where $\tilde{M} < M$, thus giving an increase in the magnitude of $\xi' v$.

APPENDIX: EXPERIMENTAL RADIATIVE WIDTHS IN ^{11}B

The new information of Moreh *et al.*[25] on total radiative widths of ^{11}B levels produces sufficient differences from previous compilations to warrant the inclusion here of our adopted values for the comparison to theory given in Table V.

Listed in Table IX are ground-state radiative widths for the particle-bound levels of ^{11}B. Combining them with the branching ratios as described in footnote b leads to the total widths given in the last column. The transition strengths of Table V are based on these results.

Results from the two particle unbound states at 9.19 and 9.27 MeV are also included in Tables V

TABLE IX. Radiative widths of levels in ^{11}B from the (γ,γ') and (e,e') data listed in Table 11.16 of Ref. 6.

E_x (MeV)	J^π (assumed)	Γ_{γ_0} (eV)[a] Moreh[c]	Average[d]	Number of measurements	Γ_γ[b] (eV)
2.12	$\frac{1}{2}^-$	0.118(13)	0.123(7)	5	0.123(7)
4.45	$\frac{5}{2}^-$	0.550(20)	0.558(18)[e]	3	0.558(18)
5.02	$\frac{3}{2}^-$	1.640(70)	1.680(56)	3	1.963(67)
6.74	$\frac{7}{2}^-$	0.021(5)	0.021(5)	1	0.030(7)
6.79	$\frac{1}{2}^+$	0.260(30)	0.260(30)	1	0.385(44)
7.29	$\frac{5}{2}^+$	0.990(70)	1.000(68)	2	1.149(80)
7.98	$\frac{3}{2}^+$	0.530(70)	0.530(70)	1	1.15(15)
8.56	$\frac{3}{2}^-$	0.530(50)	0.530(50)	1	0.946(90)
8.92	$\frac{5}{2}^-$	4.160(23)	4.150(20)	3	4.368(21)
9.19	$\frac{7}{2}^+$			3	0.31(10)
9.27	$\frac{5}{2}^+$			3	2.67(53)

[a]The ground state radiative width.
[b]The total radiative width calculated from the average $\Gamma_{\gamma 0}$ and the ground state branching ratios of Table II (if given) or Ref. 6, Table 11.4.
[c]Reference 25; note the misprint: $\Gamma_\gamma(8.559\ \mathrm{MeV}) = 1.00 \pm 0.10$ eV and not 0.66 ± 0.09 eV.
[d]The weighted average of the values listed in Table 11.16 of Ref. 6. with the data of Moreh (Ref. 25) replacing the preliminary version of that report and with systematically high (e,e') data of Kan *et al.* [Phys. Rev. C 11, 323 (1975)] omitted.
[e]The least squares average of the two measurements of the $E2/M1$ mixing ratio, δ, is $-0.197(17)$ from -0.19 ± 0.03 and -0.20 ± 0.02 (see Ref. 6). From this value of δ the partial $M1$ and $E2$ widths are calculated to be 537(18) and 20.8(37) meV, respectively.

and IX. The origin of the data for these levels is three independent measurements[40–42] of the resonance strength factor $\Gamma_\gamma\Gamma_\alpha/\Gamma$, with $\Gamma=\Gamma_\gamma+\Gamma_\alpha$, for the α resonances at 819 and 958 keV in ^{7}Li$(\alpha,\gamma)^{11}$B corresponding to the ^{11}B levels at 9.19 and 9.27 MeV, respectively. The three are in fair agreement, and the average values for $\Gamma_\gamma\Gamma_\alpha/\Gamma$ obtained are 0.280 and 2.67 eV, respectively. Uncertainties are not quoted by the authors. We estimate a 20% uncertainty for these parameters. For the 9.19-MeV level a value of $\Gamma_\gamma/\Gamma=0.1^{+0.2}_{-0.05}$ has been determined.[43] For the 9.27-MeV level $\Gamma_\alpha/\Gamma=1.0$ can be assumed. Thus, the best current total experimental radiative widths for the ^{11}B 9.19- and 9.27-meV levels are 310^{+147}_{-65} meV (we round this value off to 310 ± 100 meV) and 2.67 ± 0.53, respectively. The radiative widths of Table V are calculated using these total widths, and the branching ratios of Green *et al.*[42] quoted in the compilation of Selove.[6] Note that the γ branches given for the 9.19-MeV level do not add up to 100% because several weak branches were observed but not assigned (see also Morinaga *et al.*[44])

[1]K. Kubodera, J. Delorme, and M. Rho, Phys. Rev. Lett. 40, 755 (1978); M. Rho and G. E. Brown, Comments Nucl. Part. Phys. A 10, 201 (1981).

[2]I. S. Towner and F. C. Khanna, Nucl. Phys. A372, 331 (1981), and references contained therein.

[3]E. G. Adelberger, D. C. Hoyle, H. E. Swanson, and R. D. Von Lintig, Phys. Rev. Lett. 46, 695 (1981); W. C. Haxton, *ibid.* 46, 698 (1981).

[4]D. Kurath and W. Teeters, Phys. Lett. 101B, 5 (1981).

[5]D. J. Millener and E. K. Warburton (unpublished).

[6]F. Ajzenberg-Selove and C. L. Busch, Nucl. Phys. A336, 1 (1980).

[7]E. K. Warburton, D. E. Alburger, and D. H. Wilkinson, Phys. Rev. C 26, 1186 (1982), the following paper.

[8]D. H. Wilkinson and D. E. Alburger, Phys. Rev. 113, 563 (1959).

[9]D. E. Alburger and G. A. P. Engelbertink, Phys. Rev. C 2, 1594 (1970).

[10]D. E. Alburger and D. H. Wilkinson, Phys. Rev. C 3, 1492 (1971).

[11]D. E. Alburger, D. J. Millener, and D. H. Wilkinson, Phys. Rev. C 23, 473 (1981).

[12]D. R. Goosman and D. E. Alburger, Phys. Rev. C 5, 1252 (1972); 6, 825 (1972).

[13]G. E. Schwender, D. R. Goosman, and K. W. Jones, Rev. Sci. Instrum. 43, 832 (1972).

[14]R. A. Meyer, Lawrence Livermore Laboratory Report M-100, 1978. Additional references reported therein.

[15]E. K. Warburton and D. E. Alburger, Nucl. Instrum. Methods 178, 443 (1980).

[16]E. K. Warburton and D. E. Alburger, Phys. Rev. C 23, 1234 (1981).

[17]E. K. Warburton, G. T. Garvey, and I. S. Towner, Ann. Phys. (N.Y.) 57, 174 (1970).

[18]S. Cohen and D. Kurath, Nucl. Phys. 73, 1 (1965).

[19]J. P. Elliott and C. E. Wilsdon, Proc. R. Soc. London A272, 509 (1968); M. Harvey, Adv. Nucl. Phys. 1, 67 (1968).

[20]W. D. Teeters and D. Kurath, Nucl. Phys. A275, 61 (1977).

[21]D. J. Millener and D. Kurath, Nucl. Phys. A255, 315 (1975).

[22]W. D. Teeters and D. Kurath, Nucl. Phys. A283, 1 (1977).

[23]A. Richter, Technische Hochschule Darmstadt Report IKDA 80/15, 1980.

[24]N. Nishioka, S. Saito, and M. Yasuno, Prog. Theor. Phys. 62, 424 (1979); H. Furutani, H. Kanada, T. Kaneko, S. Nagata, H. Nishioka, S. Okabe, S. Saito, T. Sakuda, and M. Seya, Suppl. Prog. Theor. Phys. 68, 193 (1980).

[25]R. Moreh, W. C. Sellyey, and R. Vodhanel, Phys. Rev. C 22, 1820 (1980); 24, 2394 (1981).

[26]S. J. Skorka, J. Hertel, and T. W. Retz-Schmidt, Nucl. Data A2, 347 (1966).

[27]D. R. Goosman, E. G. Adelberger, and K. A. Snover, Phys. Rev. C 1, 123 (1970); D. R. Goosman and R. W. Kavanagh, *ibid.* 7, 1717 (1973).

[28]S. S. Hanna, K. Nagatani, W. R. Harris, and J. W. Olness, Phys. Rev. C 3, 2198 (1971).

[29]D. H. Wilkinson, *Nuclear Physics with Heavy Ions and Mesons,* 1977, Les Houches Lectures, edited by R. Balian, M. Rho and G. Ripka (North-Holland, Amsterdam, 1978), p. 955.

[30]H. Schopper, *Weak Interactions and Nuclear Beta Decay* (North-Holland, Amsterdam, 1966).

[31]I. S. Towner and J. C. Hardy, Nucl. Phys. A179, 489 (1972).

[32]I. S. Towner, E. K. Warburton, and G. T. Garvey, Ann. Phys. (N.Y.) 66, 674 (1971).

[33]H. Behrens and W. Bühring, Nucl. Phys. A162, 111 (1971).

[34]D. H. Wilkinson, Nucl. Phys. A377, 474 (1982).

[35]D. M. Brink and G. R. Satchler, *Angular Momentum* (Clarendon, Oxford, 1968).

[36]R. J. Blin-Stoyle and S. C. K. Nair, Adv. Phys. 15, 493 (1966).

[37]H. A. Smith and P. C. Simms, Phys. Rev. C 1, 1809 (1970).

[38]J. Damgaard and A. Winther, Phys. Lett. 23, 345

(1966).
[39]C. M. Shakin, private communication.
[40]W. E. Bennett, P. A. Roys, and B. J. Toppel, Phys. Rev. 82, 20 (1951).
[41]G. A. Jones, C. M. P. Johnson, and D. H. Wilkinson, Philos. Mag. 4, 796 (1969).
[42]L. L. Green, G. A. Stephens, and J. G. Wilmott, Proc. Phys. Soc. London 79, 1017 (1962).
[43]J. W. Olness, E. K. Warburton, D. E. Alburger, and J. A. Becker, Phys. Rev. 139, B512 (1965).
[44]H. Morinaga, L. Leoni, M. Morando, C. Signorini, G. Fortuna, and B. Delaunay, *Proceedings of the International Conference on Nuclear Structure, Tokyo, 1977,* edited by T. Marumori (Physical Society of Japan, Tokyo, 1978), contributed papers, p. 156.